

Vibration analysis of mountain tunnel lining built with forepoling method

Yang Gao^{*1,2}, Yujing Jiang³, Yanliang Du¹, Qian Zhang¹ and Fei Xu¹

¹Key Laboratory of Structural Health Monitoring and Control, Shijiazhuang Tiedao University, Shijiazhuang 050043, China

²State Key Laboratory of Geomechanics and Geotechnical Engineering, Institute of Rock and Soil Mechanics, Chinese Academy of Sciences, Wuhan, 430071, China

³Graduate School of Engineering, Nagasaki University, Nagasaki 852-8521, Japan

(Received December 2, 2017, Revised March 15, 2018, Accepted March 27, 2018)

Abstract. Nowadays, many tunnels have been commissioned for several decades, which require effective inspection methods to assess their health conditions. The ambient vibration test has been widely adopted for the damage identification of concrete structures. In this study, the vibration characters of tunnel lining shells built with forepoling method was analyzed based on the analytical solutions of the Donnell-Mushtari shell theory. The broken rock, forepoling, rock-concrete contacts between rock mass and concrete lining, was represented by elastic boundaries with normal and shear stiffness. The stiffness of weak contacts has significant effects on the natural frequency of tunnel lining. Numerical simulations were also carried out to compare with the results of the analytical methods, showing that even though the low nature frequency is difficult to distinguish, the presented approach is convenient, effective and accurate to estimate the natural frequency of tunnel linings. Influences of the void, the lining thickness and the concrete type on natural frequencies were evaluated.

Keywords: tunnel lining; Donnell-Mushtari shell theory; natural frequency; elastic support

1. Introduction

Japan is a country surrounded by sea and 70% of its land is covered by mountains. A large number of tunnels have been constructed in mountainous areas during the last several decades, and those tunnels have become an indispensable part of the national traffic networks. The persistent ageing of tunnels causes many problems on the lining of tunnel, such as corrosion, buckling, fracturing, generation of internal voids and seepage (Malmgren *et al.* 2005). Deteriorations and damages of lining concrete decrease the integrity of tunnel lining and subsequently affect the workability, serviceability and safety reliability of tunnels (Aktan *et al.* 2000, Bhalla *et al.* 2005). Therefore, appropriate inspection needs to be conducted at appropriate time to ensure the effective function of tunnel.

To date, a number of inspection methods including destructive and nondestructive approaches have been proposed and used in practices to evaluate concrete structure integrities (Ni *et al.* 2010, 2012). However, these methods can only provide localized information and require considerable time and cost to estimate overall tunnel integrity (Park and Choi 2008). With the development and application of high sensitivity accelerometer, the low-cost ambient vibration test has attracted much more attentions for evaluating the structural condition of the whole structure of tunnel lining. Therefore, it is important to study the analytical solutions of tunnel lining vibrations with appropriate models in order to improve the understanding of

their dynamic behaviors.

A mountain tunnel lining can be treated as a thin cylindrical shell structure of which the thickness is much smaller than other dimensions. The vibration of thin elastic shells has been studied by many researchers and numerous different shell theories have been derived in the literature (e.g., Love 1888, Timoshenko 1959, Lur'ye 1940). The main differences among these theories are the various assumptions about the form of terms with small magnitude (e.g., small displacement) and the order of these terms. Various thin cylindrical shells with ideal boundary conditions, e.g., clamped, free, simply supported with axial constraint and simply supported without axial constraint were analyzed in these studies.

A variety of methods have been applied to the study of thin shell vibration. Approximate analyses based on various shell theories have been performed using the Rayleigh-Ritz method (Leissa 1973). Exact solution of wave propagation in infinite cylinders has also been widely used for the thin shell vibrations with different boundary conditions (Aremenakas *et al.* 1969, Harari 1978, Fuller 1981).

In recent years, the train-induced vibration of railway tunnels and its propagation in the ground have been studied with both analytical and numerical methods, which focus on the ground-borne vibrations transmitting to the adjacent structures. The influence of the vibration source (the moving train) and the propagation path (the composition of the ground) of wave are mainly discussed. In order to simplify the modeling process, the ground is to be continuously bonded to the outer surface of the tunnel, and the tunnel-ground interface is usually neglected. Displacement and strain is usually treated as compatible at the interface boundaries (Metrikine *et al.* 2000). Few

*Corresponding author, Associate Professor
E-mail: gaoyang_sjz@163.com

attentions have focused on the vibration characteristics of tunnel itself, especially with the low amplitude ambient vibrations evoked by vehicle in tunnel (Gao *et al.* 2012). In those old mountain tunnels built with forepoling method, completely contact boundary conditions are hardly achieved and flexibility supports usually exist between the rock and the tunnel lining.

In this study, the Donnell-Mushtari shell theory is adopted and extended to the elastic boundary conditions to analyze the vibration characters of tunnel lining built with forepoling method. The rock-concrete contacts between rock mass and concrete lining, is considered as elastic boundaries which can be represented by the distributed springs between the rock and the tunnel shell lining. It is found that the stiffness of elastic supports has significant effect on the natural frequency of the lining. This stiffness can also be estimated by natural frequencies of tunnel lining. Numerical results are compared with analytical solutions proposed in this study and good agreement is found.

2. Theoretical formulation

A mountain tunnel can be considered as an infinite cylindrical shell structure with the similar elastic supports between the surrounding ground and the lining shell. Hence, a plane strain model of the cylindrical shell is adopted, as shown in Fig. 1. Vibration modes in cross section of the shell are mainly discussed.

2.1 Donnell–Mushtari shell Equations

The equations of motion for tunnel shell in plane strain state can be written using Donnell and Mushtari theory, which have been used most widely in the simplified shell vibrations.

$$\frac{K}{R^2} \frac{\partial^2 v}{\partial \theta^2} + \frac{K}{R^2} \frac{\partial w}{\partial \theta} = \rho h \frac{\partial^2 v}{\partial t^2} \tag{1a}$$

$$-\frac{K}{R^2} \frac{\partial v}{\partial \theta} - \frac{K}{R^2} w - k \frac{K}{R^2} \frac{\partial^4 w}{\partial \theta^4} = \rho h \frac{\partial^2 w}{\partial t^2} \tag{1b}$$

where $k = h^2 / (12 R^2)$, $K = E h / (1 - \mu^2)$, r and θ are the polar coordinates, v and w the orthogonal components of displacement of the shell (Fig. 1), ρ is the density, E is Young’s modulus of elasticity, μ is Poisson’s ratio, h is the thickness of lining shell, R is the radius of the neutral plane and t is time. Due to the damping of concrete is relatively small, the actual vibration modes approximate undamped natural modes quite well inside usual limits of experimental accuracy (Soedel 2004). The damping effects is not included in motion equations.

In the old tunnels that were built with the forepoling method, the wooden poling board was used instead of shotcrete so that incomplete contacts usually exist between rock mass and poling board, as shown in Fig. 2. Under the long-term weather and ground compression, the wooden board has been pressed into crack thin plate. The unbounded contacts, poling board and the loosening zone of surrounding rockmass can be simplified to weak interfaces

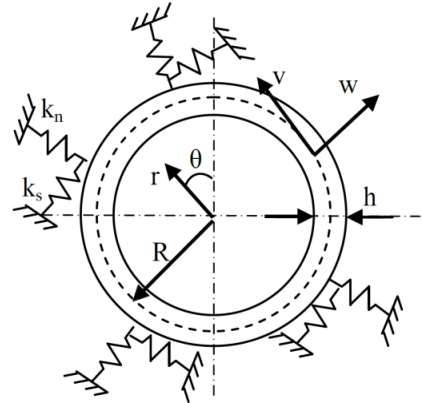


Fig. 1 The schematic diagram of a circular cylindrical shell

which can be represented by the distributed springs with the low normal stiffness k_n and the shear stiffness k_s . The elastic foundation boundary included in shell theory is defined through the additional load terms q_r and q_θ as (neglecting damping effects):

$$q_\theta = -k_s v \tag{2a}$$

$$q_r = -k_n w \tag{2b}$$

Eqs. (1) therefore becomes

$$\frac{K}{R^2} \frac{\partial^2 v}{\partial \theta^2} + \frac{K}{R^2} \frac{\partial w}{\partial \theta} - k_s v = \rho h \frac{\partial^2 v}{\partial t^2} \tag{3a}$$

$$-\frac{K}{R^2} \frac{\partial v}{\partial \theta} - \frac{K}{R^2} w - k \frac{K}{R^2} \frac{\partial^4 w}{\partial \theta^4} - k_n w = \rho h \frac{\partial^2 w}{\partial t^2} \tag{3b}$$

The displacements of the shell can be expressed in the form of wave propagation as follows

$$v = V e^{j\omega t} = B \sin n\theta e^{j\omega t} \quad (n=0,1,2,\dots) \tag{4a}$$

$$w = W e^{j\omega t} = C \cos n\theta e^{j\omega t} \tag{4b}$$

where B and C are the amplitudes of the displacement in r and θ directions, and ω is the natural frequency. Substituting the displacements corresponding v and w in to Eqs. (3) gives

$$\frac{K}{R^2} \frac{\partial^2 V}{\partial \theta^2} + \frac{K}{R^2} \frac{\partial W}{\partial \theta} - k_s V + \rho h \omega^2 V = 0 \tag{5a}$$

$$\frac{K}{R^2} \frac{\partial V}{\partial \theta} + \frac{K}{R^2} W + k \frac{K}{R^2} \frac{\partial^4 W}{\partial \theta^4} + k_n W - \rho h \omega^2 W = 0 \tag{5b}$$

This system of equations can be written in matrix form and the determinant of the matrix must be zero for non-trivial solutions as follows

$$\begin{vmatrix} n^2 + \frac{R^2}{K} k_s - \Omega^2 & n \\ n & 1 + kn^4 + \frac{R^2}{K} k_n - \Omega^2 \end{vmatrix} = 0 \quad (n=0,1,2,\dots) \tag{6}$$

The frequency factor Ω can be obtained

$$\Omega^2 = 1 + \frac{R^2}{K} k_n \quad (n=0) \tag{7a}$$

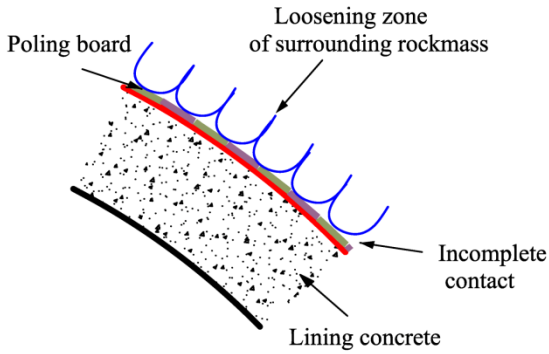


Fig. 2 The cross section of the tunnel lining built by the poling-board method

$$\Omega^2 = \frac{1}{2} \left[1 + \frac{R^2}{K} k_n + \frac{R^2}{K} k_s + n^2 + kn^4 \right] \pm \frac{1}{2} \sqrt{\left[1 + \frac{R^2}{K} k_n + \frac{R^2}{K} k_s + n^2 + kn^4 \right]^2 + 4n^2 - 4 \left(n^2 + \frac{R^2}{K} k_s \right) \left(1 + kn^4 + \frac{R^2}{K} k_n \right)} \quad (n \neq 0) \quad (7b)$$

2.2 The natural frequency influenced by the void

Voids, usually existing between concrete linings and rock masses (see Fig. 3), are unfavorable to the supporting system and may invoke lining structure failures, such as water leakage, reinforcement corrosion and cracking. They can induce increased deformation and stresses in the close vicinities, which are one of the main sources that cause serious damages on tunnel linings. Meanwhile, the existence of the void changes the elastic foundation boundary into the free boundary on the outer surface of tunnel lining. At here, outer surface stands for the surface of lining closer to the void. Here, the void is considered as the additional distribution load which is equivalent in magnitude to the elastic boundary load but opposite in direction acting on the outer surface.

$$q_{v\theta} = k_s v \quad (8a)$$

$$q_{vr} = k_n w \quad (8b)$$

where $q_{v\theta}$ and q_{vr} are the additional distribution load in θ and r direction to represent the existence of the void.

The motion equations can be rewritten as

$$\frac{K}{R^2} \frac{\partial^2 v}{\partial \theta^2} + \frac{K}{R^2} \frac{\partial w}{\partial \theta} - k_s v - \rho h \frac{\partial^2 v}{\partial t^2} = -k_s v \delta(\theta) \quad (9a)$$

$$-\frac{K}{R^2} \frac{\partial v}{\partial \theta} - \frac{K}{R^2} w - k \frac{K}{R^2} \frac{\partial^4 w}{\partial \theta^4} - k_n w - \rho h \frac{\partial^2 w}{\partial t^2} = -k_n w \delta(\theta) \quad (9b)$$

where $\delta(\theta) = \begin{cases} 1 & -\gamma/2 \leq \theta \leq \gamma/2 \\ 0 & \text{else} \end{cases}$

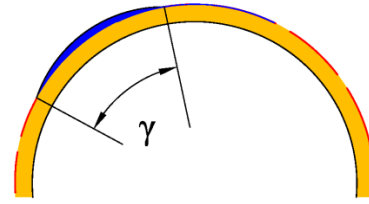


Fig. 3 Schematic view of a void at rock-concrete interface. void arc length: sector angle γ

As the natural frequency have been analyzed in Section 2.1, the influence of the additional load on the frequencies can be estimated by the modal expansion approach. The displacement of continuous systems can be written in an infinites series as

$$v(\theta, t) = \sum_{n=1}^{\infty} \eta_n(t) V \quad (10a)$$

$$w(\theta, t) = \sum_{n=1}^{\infty} \eta_n(t) W \quad (10b)$$

where η_n is the modal participation factor. In this type of tunnel lining built with forepoling method, the void induces a major decrease of the 1st-order natural frequency, and the void can be identified based on changes of the 1st-order natural frequency (Jiang *et al.* 2014). Hence, influences of the void on 1st-order natural frequency is analyzed in following. The lining shell section where the void exists can be regarded as a slightly curved plated, of which 1st-order mode is associated primarily with transverse motion. Therefore, only the vibration in the radial direction is considered. Substituting in Eq. (9(b)) gives

$$\sum_{n=1}^{\infty} \left[\left(\frac{K}{R^2} \frac{\partial V_n}{\partial \theta} + \frac{K}{R^2} W_n + k \frac{K}{R^2} \frac{\partial^4 W_n}{\partial \theta^4} + k_n W_n \right) \eta_n + \rho h \eta_n \right] W_n = k_n \delta(\theta) \eta_n W_n \quad (11)$$

Based on the eigenvalue analysis, it has been know that

$$\frac{K}{R^2} \frac{\partial V_n}{\partial \theta} + \frac{K}{R^2} W_n + k \frac{K}{R^2} \frac{\partial^4 W_n}{\partial \theta^4} + k_n W_n = \rho h \omega_n^2 W_n \quad (12)$$

where ω_n is the natural frequency of tunnel lining without voids. Substituting this in Eq. (11) gives

$$\sum_{n=1}^{\infty} \left(\rho h \omega_n^2 \eta_n + \rho h \eta_n \right) W_n = k_n \delta(\theta) \eta_n W_n \quad (13)$$

Since the vibration modes W_n are orthogonal, Eq. (13) can be written by multiplying with a mode W_p where p is either equal to n or not equal

$$\left(\rho h \omega_n^2 \eta_n + \rho h \eta_n \right) W_n^2 = k_n \delta(\theta) \eta_n W_n^2 \quad (14)$$

Integrating over the lining shell and substituting Eq. (4(b)) gives

$$\eta_n + \omega_n^2 \eta_n = \frac{\eta_n}{\rho h N_n} \int_{-\gamma/2}^{\gamma/2} k_n \cos^2 n\theta R d\theta \quad (15)$$

where $N_n = \int_0^{2\pi} \cos^2 n\theta R d\theta$

Therefore, the natural frequencies ω_{vn} , which are affected by the void, can be calculated as

$$\omega_{vn} = \sqrt{\omega_n^2 - \frac{1}{\rho h N_n} \int_{-\gamma/2}^{\gamma/2} k_n \cos^2 n\theta R d\theta} \quad (16)$$

3. Numerical simulations and discussions

3.1 Numerical simulations of tunnel vibrations

To verify the analysis discussed above, numerical simulations were performed by using the Distinct Element Method (DEM) code of UDEC to investigate the natural frequency of tunnel lining.

In numerical simulations, The unbounded contacts, poling board and the loosening zone of surrounding rockmass can be represented by the interface element with low normal and shear stiffness, which are treated as discontinuities between distinct bodies (i.e., the discontinuity is treated as an inner boundary in the DEM) (UDEC 2000). The Mohr-Coulomb model and Coulomb slip model were adopted to represent the mechanical behavior of rock masses and interfaces, respectively. Those types of elements can effectively simulate the dynamic deformational behavior of rock mass, lining concrete and interfaces. The shape and size of the numerical model are shown in Fig. 4. The physic-mechanical properties of the surrounding rock mass, lining concrete and concrete-rock interfaces are listed in Table 1, which are determined according to the rock mass and concrete lining of a tunnel in Japan.

A stationary Gaussian white noise with a frequency range from 0 to 100 Hz was input on the floor of tunnel to represent the exciting source (e.g., passing vehicles). The element size was set to be 0.2 m in order to simulate the propagation of stress waves accurately. The damping ratio was set to 0 during dynamic calculations. The boundaries of model were set as viscous boundaries to minimize wave reflections at boundaries. The vibration histories of the lining surface in both the horizontal direction and the vertical direction were recorded to obtain the natural frequencies. 32768 discrete time signal data at the monitoring point were recorded during numerical simulations with a sampling interval of 0.001s.

In order to find the natural frequencies, the power spectrum of vibration histories recorded on the surface of tunnel lining were calculated and normalized by

$$NPSD(f) = P(f) / \sqrt{\sum_{k=1}^m P(f)^2} \quad (17)$$

where $P(f)$ the Power Spectrum Density (PSD), $NPSD(f)$ is the normalized PSD corresponding to the frequency f and k is the number of frequency points. One typical example was shown in Fig. 5, and the corresponding mode shapes were plotted in Fig. 6. The natural frequencies can be identified by the peak-picking method, even though the frequency peak around 46.31 Hz are not as obvious as others. The first

four order natural frequencies were picked and compared to the results of Eqs. (7) as shown in Fig. 7, and the first four modes were listed in Table 2.

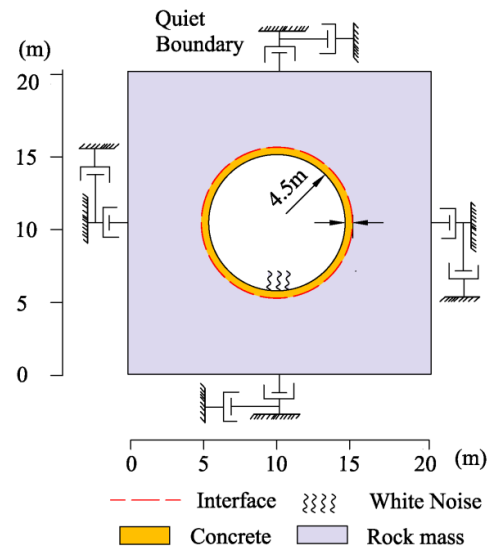


Fig. 4 Model of numerical simulation

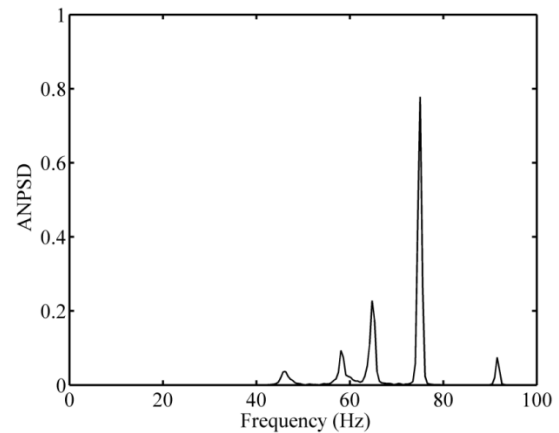


Fig. 5 The normalized power spectrum of vibration on the surface of tunnel lining

Table 1 Material properties used in the numerical simulations

Parameters		Units	Values
Intact rock	Density	kg/m ³	2550
	Elastic modulus	GPa	30
	Poisson ratio	-	0.22
Concrete	Density	kg/m ³	2500
	Elastic modulus	GPa	22
	Poisson ratio	-	0.28
Interface	Normal stiffness	MPa/m	200
	Shear stiffness	MPa/m	20

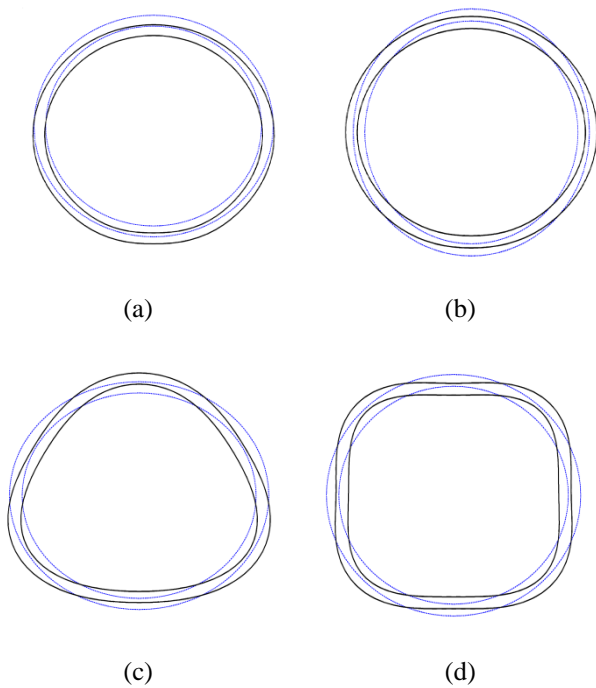


Fig. 6 Calculated mode shapes. (a) 46.31 Hz, (b) 58.25 Hz, (c) 64.93 Hz and (d) 74.96 Hz

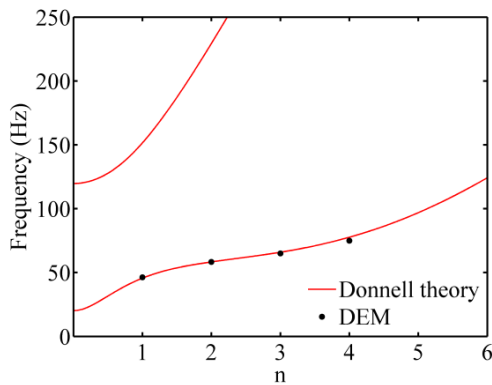


Fig. 7 The natural frequencies of analytical solution and DEM simulation

In the Donnell theory, two nonzero sets of natural frequencies can be confirmed. Low-order natural frequencies, which can be excited easily, are widely adopted in modal analysis for the damage identification. Hence, the natural frequencies bellow 100 Hz was analyzed primarily due to the accuracy limitations of measurements. In this study, A relative error parameter in Table 2 is defined as following

$$Error = \frac{f_{theory} - f_{DEM}}{f_{DEM}} \times 100\% \quad (18)$$

The errors of the frequencies in Table 2 are very small (less than 3%), so the proposed approach is correct and its results are considered to be reliable and accurate.

In the thin shell theory, the transverse shear deformation

in shell-bending behavior is ignored. As the thickness-to-radius ratio increases, the shear deformation tends to be significant. The influence of h/R on the natural frequency error was plotted in Fig. 8. The error of each vibration mode increases with the increment of h/R except $n = 1$. For $n \leq 2$, the error is relatively small in all cases (below 3%), which indicates that h/R has few influence on low frequency modes. While for $n = 4$, the error increases greatly with the increment of h/R . Therefore, the thick shell theory is recommended to adopted to give a accurate result for high frequency modes when $h/R > 0.1$.

3.2 Influence of the void on the natural frequency

A series of simulation models with the simplified circular void between rock mass and tunnel lining where voids usually exist, were simulated to verify the analytical results calculated by the modal expansion approach. Their natural frequencies and the mode shapes are plotted in Figa. 9 and 10.

In both the analytical and DEM results, the natural frequencies decrease with the increment of the void size (defined by sector angle γ). The significant influence of the void size exists in the first order frequency, and the variation declines in higher modes.

For $n = 1$, vibrations in the radial direction are induced primarily (Fig. (10a)), which agrees with the assumption in Section 2.2. Hence the frequency errors defined in Eq. (11) are very tiny (less than 0.5%). While for $n \geq 2$, the errors increase (still less than 3%). It is because the circumferential deflections, which are ignored in Eq. (11), increase in the higher order mode. However, the proposed approach can still be viewed as a proper method for the estimation of the first order frequency of the lining with the void.

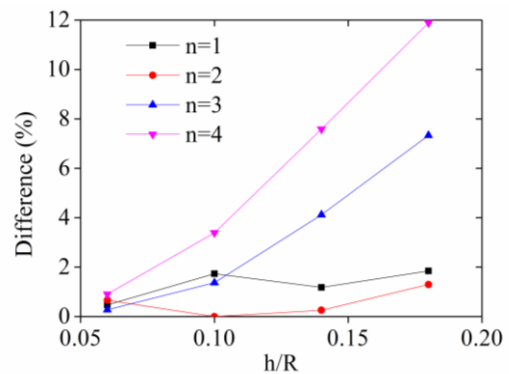


Fig. 8 Influence of h/R on nature frequency error

Table 2 Comparison of natural frequencies

n	DEM (Hz)	Donnell theory (Hz)	Error (%)
1	46.31	45.52	2
2	58.25	58.25	0
3	64.93	65.83	1
4	74.96	77.59	3

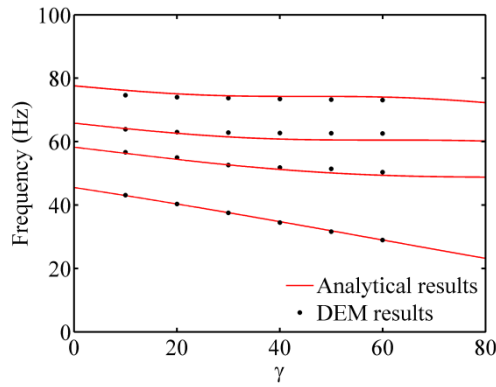


Fig. 9 The nature frequencies influenced by the void sector angle

3.3 Influence of the rock-concrete interface stiffness on the natural frequency

The supporting system has a great influence on the natural frequency of a structure, and the decrease of the contact stiffness between the rock mass and the lining will reduce the natural frequency of the system (Chowdhury 1990). The influence of the interface stiffness on the natural frequency is illustrated in Fig. 11.

The natural frequencies increase with stiffness, and the significant increase exists in the low natural frequencies (vibration modes of $n = 1, 2, 3$), as shown in Fig. 11(a). Due to the shear stiffness is much less than normal stiffness, the natural frequencies are mainly affected by the normal stiffness.

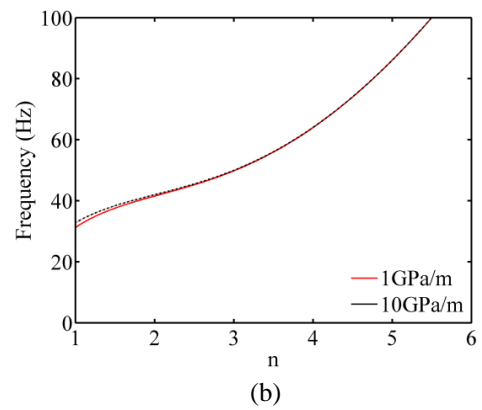
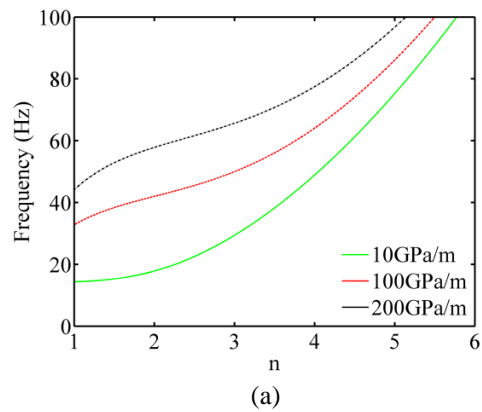


Fig. 11 Influence of concrete-rock interfaces on natural frequencies. (a) Natural frequencies corresponding to different normal stiffness of concrete-rock interfaces (the shear stiffness is 10 GPa/m.) and (b) Natural frequencies corresponding to different shear stiffness of concrete-rock interfaces (the normal stiffness is 100 GPa/m)

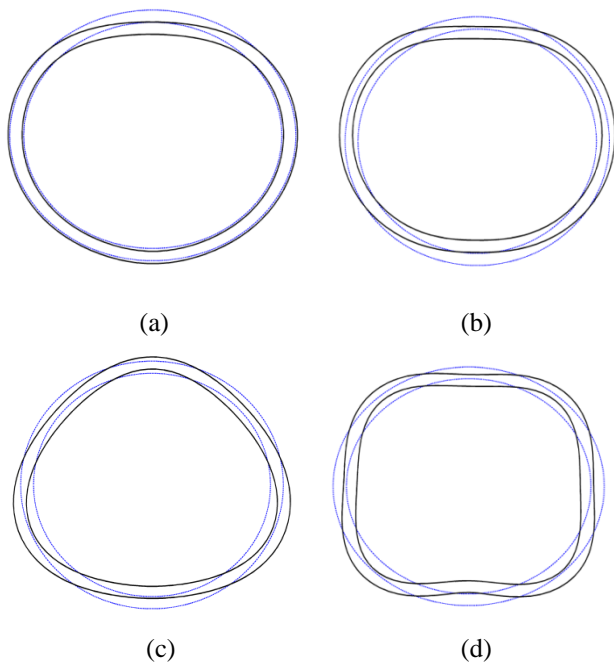


Fig.10 One group of calculated mode shapes with the void sector angle of 60 °. (a) 28.98 Hz, (b) 50.40 Hz, (c) 62.61 Hz and (d) 73.11 Hz

There is almost no variation of frequencies when the shear stiffness changes (Fig. 11(b)). It is difficult to directly measure the exact stiffness of concrete-rock interfaces through traditional mechanical testing; nevertheless, the natural frequency measuring provides a new approach to estimate that stiffness.

4. Discussion

In the Donnell-Mushtari Equations, the bending and membrane effects are neglected. The simplifications agree well with the vibration modes of $n = 1, 2$ (Figs. 6(a) and 6(b)). Therefore, these natural frequencies estimated by Donnell theory are accurate and their errors are less than 2% (Fig. 8). Theoretically the errors increase with the h/R , while the error decrease firstly when $n=2$ in Fig. 8. This might be caused by the DEM simulations. The accuracy of the natural frequencies calculated by DEM is influenced by the element size, the material property, the sampling period & interval and so on. The inaccurate of the DEM results would induce the error of the natural frequency in the vibration mode ($n=2$) decreases firstly. A further study with the refined model will be carried out in future to verify this

opinion.

In-situ microtremor measurements of a tunnel lining were carried out on the Satomi tunnel located in Sasebo City, Nagasaki Prefecture, Japan (Gao *et al.* 2012). According to the tunnel inspection results, two typical spans with different health conditions were chosen for microtremor measurements. one is the healthy span, and the other is the span with voids.

The power spectrum of the measured signals was calculated. The first three order natural frequencies (56.6 Hz, 78.1 Hz and 86.9 Hz) were identified in healthy span, while six natural frequencies (32.2 Hz, 68.4 Hz, 74.2 Hz, 78.1 Hz, 83.1 Hz and 88.9 Hz) were in that span with voids. The normal stiffness of the rock-concrete interface can be estimated by the natural frequencies of the healthy span based on the numerical simulation method mentioned in this manuscript. The in-situ measurement results also verified the existence of the voids induces a decrement of the first order natural frequency. The theoretical study proposed in Section 2 also give a theoretical explanation for the variation of the frequency peaks of tunnel lining microtremors.

5. Conclusions

The nature frequencies of tunnel lining shell with the supporting of elastic rock-concrete interfaces were analyzed based on the Donnell-Mushtari shell theory. The accuracy and validity of proposed approach in the plane strain model were confirmed by comparison with the results of DEM numerical simulations.

- The natural frequency of the thin shell can be estimated accurately by the proposed approach in this study. As the thickness-to-radius ratio increases ($h/R > 0.1$), the frequency error trends to be significant especially in high mode ($n > 3$) and a thick shell theory is recommended.
- The natural frequencies decrease with the increment of the void size and the significant influence of the void size exists in the first order frequency. The first order natural frequency can be estimated accurately.
- The elastic rock-concrete interface has a great influence on natural frequencies of the tunnel lining. For $n \geq 1$, the nature frequencies are mainly affected by the normal stiffness. The interface stiffness has the largest influence on low nature frequencies in vibration modes of $n = 1, 2, 3$. The tunnel lining shell frequency measurement also provides a new approach to estimate the interface stiffness

Acknowledgments

This work was partly supported by Cooperative Innovation Center of Disaster Prevention and Mitigation for Large Infrastructure in Hebei province (Shijiazhuang Tiedao University), National Natural Science Foundation of China (No. E080506), China Postdoctoral Science Foundation (2017M610170) and Open Research Fund of

State Key Laboratory of Geomechanics and Geotechnical Engineering, Institute of Rock and Soil Mechanics, Chinese Academy of Sciences, Grant NO Z017001. The authors would like to thank Assistant Professor Bo Li in Graduate School of Engineering of Nagasaki University in Japan for his kind support and advice in this research.

References

- Aktan, A.E., Catbas, F.N., Grimmelman, K.A. and Tsikos, C.J. (2000), "Issues in infrastructure health monitoring for management", *J. Eng. Mech. - ASCE*, **126**, 711-724.
- Aremenakas, A.E., Gazis, D. and Herrmann, G. (1969), *Free vibration of Circular Cylindrical Shells*. Pergamon Press, Oxford.
- Bhalla, B.S., Yang, Zhao, Y.W. and Soh, C.K. (2005), "Structural health monitoring of underground facilities - Technological issues and challenges", *Tunn. Undergr. Sp. Tech.*, **20**, 487-500.
- Blevins, R.D. (1979), *Formulas for Natural Frequency and Mode Shape*. Van Nostrand Reinhold, New York.
- Chowdhury, M.R. (1990), "Experimental modal testing and analysis of continuously supported structures", *Proceedings of the 8th International Modal Analysis Conference*, Florida, February 1990.
- Fuller, C.R. (1981), "The effect of wall discontinuities on the propagation of flexural waves in cylindrical shells", *J. Sound Vib.*, **75**, 207-228.
- Gao, Y., Jiang, Y., Li, B., Ogawa, Y. and Yang, L. (2012), "Research on health assessment technique of tunnel lining based on power spectrum density characteristics of microtremors", *J. JSCE Division F1.*, **68**(1), 111-118.
- Harari, A. (1978), "Wave propagation in a cylindrical shell with joint discontinuity", *J. Shock Vib.*, **48**, 53-61.
- Jiang, Y., Gao, Y. and Li, B. (2014), "Estimation of effect of voids on frequency response of mountain tunnel lining based on microtremor method", *Tunn. Undergr. Sp. Tech.*, **42**, 184-194.
- Leissa, A.W. (1973), *Vibration of shells*. Washington: NASA SP-288.
- Love, A.E.H. (1888), "The small free vibrations and deformations of a thin elastic shell", *Philos. T. R. Soc. London, Ser. A*, **179**, 491-546.
- Loveday, P.W. (1998), "Free vibration of elastically supported thin cylinders including gyroscopic effects", *J. Sound Vib.*, **217**, 547-562.
- Lur'ye, A.I. (1940), "General theory of elastic shells", *Prikladnaya Matematika i Mekhanika*, **4**, 7-34.
- Malmgren, L., Nordlund, E. and Rolund, C. (2005), "Adhesion strength and shrinkage of shotcrete", *Tunn. Undergr. Sp. Tech.*, **20**, 33-48.
- Metrikine, A.V. and Vrouwenvelder, A.C. (2000), "Surface ground vibration due to a moving train in a tunnel: two-dimensional model", *J. Sound Vib.*, **234**, 43-66.
- Ni, Y.Q., Ye, X.W. and Ko, J.M. (2010), "Monitoring-based fatigue reliability assessment of steel bridges: analytical model and application", *J. Struct. Eng. - ASCE*, **136**(12), 1563-1573.
- Ni, Y.Q., Ye, X.W. and Ko, J.M. (2012), "Modeling of stress spectrum using long-term monitoring data and finite mixture distributions", *J. Struct. Eng. - ASCE*, **138**(2), 175-183.
- Park, S. and Choi, S. (2008), *Development of methodology for estimating the effective properties of containment buildings*. Mid-term Report. Korea Institute of Nuclear Safety, KINS/HR-836.
- Soedel, W. (2004), *Vibrations of Shells and Plates*, third ed., Marcel Dekker, Inc.
- Timoshenko, S. (1959), *Theory of Plates and Shells*. McGraw-Hill,

New York.
UDEC - user's manual. Minneapolis, 2000, MN: Itasca Consulting
Group Inc.